scientific reports

Check for updates

OPEN

Assessment of stable carbon isotope ratios and source characterization of aerosols in ambient $PM_{2.5}$ from the Indian COALESCE network

Debajyoti Paul[1]✉, Gyanesh Kumar Singh[2,3]✉, Tarun Gupta[2], Abhijit Chatterjee[4], Binoy K Saikia[5], Ramya Sunder Raman[6], Gazala Habib[7], Harish Phuleria[8] & Chandra Venkataraman[9]

This study explores the potential of stable carbon isotope ($\delta^{13}C$) composition of ambient carbonaceous aerosols in assessing the nature and apportionment of their sources. As part of the CarbOnaceous AerosoL Emissions, Source apportionment & ClimatE Impacts (COALESCE) network, $\delta^{13}C$ measurements ($n = 1120$) were conducted on aerosol samples collected from eight key locations spread across India. The $\delta^{13}C$ values of aerosols exhibit distinct spatial/temporal isotopic variabilities between background and polluted (urban) sites, and indicate an origin primarily from C_3-biomass, fossil fuels, vehicular emission sources, etc. Spatial $\delta^{13}C$ distribution over India shows more negative $\delta^{13}C$ values in all seasons at the north Indian Himalayan (Kashmir) and east Indian sites (Jorhat) compared to other locations, implying that anthropogenic inputs contribute to more isotopic variability and a typical ^{13}C-rich signature. Our study shows that although $\delta^{13}C$ provides qualitative information on source characteristics, it is not a robust standalone proxy for such applications. We conclude that $\delta^{13}C$ of aerosols could be a robust proxy for quantification studies if the extent of isotopic fractionation involved during aerosol formation/transport processes is well known and if it is assessed with one or more chemical markers like radiocarbon ($\Delta^{14}C$), trace elements/organic species, and specific biomarkers (e.g., levoglucosan or K^+_{BB}).

Keywords Stable isotope, Carbonaceous aerosols, Source signature, Fractionation, Aerosol proxy

Atmospheric particulate matter (PM) is a complex mixture of organic and inorganic substances suspended in the air and has significant impacts on the environment, and in turn on human health[1–7]. Therefore, evaluation and understanding of PM sources are essential for the development of effective strategies to mitigate their adverse effects. Carbonaceous aerosols (CA) are an important component of PM playing a major role in perturbing Earth's radiative balance and thereby affecting atmospheric chemistry and climate at both long- and short-term scales[8–12]. Carbonaceous aerosols can constitute a major fraction (~30–70%) of total aerosol mass depending on the location and emission sources and therefore can significantly affect the local climate and air quality[13]. These aerosols exhibit varying chemical, physical and optical properties, and are primarily present in continental and urban tropospheric environments. Identifying and understanding their sources remains a significant

[1]Department of Earth Sciences, Indian Institute of Technology Kanpur, Kanpur 208 016, India. [2]Department of Civil Engineering and APTL at Center for Environmental Science and Engineering (CESE), Indian Institute of Technology Kanpur, Kanpur 208 016, India. [3]Air Quality and Aerosol Metrology (AQAM) Group, National Physical Laboratory (NPL), Teddington, London TW11 0LW, UK. [4]Department of Chemical Sciences, Bose Institute, Block-EN, Sector-V, Salt Lake, Kolkata 700091, India. [5]Coal & Energy Group, Coal Energy & Materials Sciences Division, CSIR North-East Institute of Science & Technology, Jorhat 785006, India. [6]Department of Earth and Environmental Sciences, Indian Institute of Science Education and Research Bhopal, Bhopal 462066, India. [7]Department of Civil Engineering, Indian Institute of Technology Delhi, New Delhi 110 016, India. [8]Environmental Science and Engineering Department, Indian Institute of Technology Bombay, Mumbai 400076, India. [9]Department of Chemical Engineering, Indian Institute of Technology Bombay, Mumbai 400076, India. ✉email: dpaul@iitk.ac.in; gyanesh.singh@npl.co.uk

challenge[14–17]. Globally, approximately 75% of CA is contributed by South and East Asian regions because of an increase in anthropogenic emissions over the past few decades related to rapid development[18–22]. Particularly, the concentration of CA in the Indian subcontinent in the last few decades has increased significantly due to a variety of factors related to economic growth[23–25], which in turn has affected atmospheric chemistry and become a major concern of deteriorating human health in the region[26–28]. The typical sources of CA in this region include biomass/bio-fuel combustion, vehicular emissions, construction/road dust, secondary PM formation, and industrial emissions[18,19]. Compared to other regions, emissions from biomass (post-harvest crop residue) burning and coal combustion (thermal power plants and brick kilns) are the major contributors of CA in the Indian subcontinent[19,27]. The subcomponents of CA are organic carbon (OC) and elemental carbon (EC) or black carbon (BC) which together constitute the total carbon (TC) fraction of ambient aerosols; EC or BC nomenclature is based on the method of determination by thermo-optical or optical properties, respectively. These components (OC and EC) possess distinct light absorption properties and have the potential to affect the Earth's radiative balance[29–32]. The EC fraction typically originates due to incomplete combustion of fossil fuel or biomass. The TC fraction also contains numerous polar and non-polar compounds such as phenols, isoprene, humic acids, polycyclic aromatic hydrocarbons (PaHs), and carbonyls etc., which play different roles in the ambient atmospheric chemistry depending on existing meteorological conditions[33–35]. However, the real impact of carbonaceous aerosols on climate and health is still ambiguous due to the existing uncertainties related to their sources, chemical composition and properties, and formation mechanisms.

Traditional chemical analyses performed on filter-based PM, such as ionic species abundances determined by ion chromatography, OC and EC concentrations by carbon analyzer, and PM mass by gravimetry provide information on pollution levels and likely sources[36,37]. In the past decade, several studies have demonstrated the potential of stable carbon ($\delta^{13}C$) and nitrogen ($\delta^{15}N$) isotope composition of aerosols to trace the nature of pollution sources and their contribution to PM, and to understand the reaction mechanisms related to the secondary formation and atmospheric aging and their control on the atmospheric chemistry, etc[38–48]. The aerosol research community has extensively used the $\delta^{13}C$ of PM to shed light on the sources and transformations of emissions[49–64]. Several authors have attempted to use carbon isotopic composition for the characterization of biomass-burning products[65–73]. Furthermore, $\delta^{13}C$ of various phases (gas and particulate) has been used to understand transformation mechanisms (gas to particle phase) and coupled with $^{14}C/^{12}C$ ratio measurements ($\Delta^{14}C$; modern biomass/biofuel sources have a value > 0‰ due to bomb-spike-origin ^{14}C in late 1950s because of nuclear weapon testing, whereas fossil fuel sources have a value of -1000‰) to quantify the contribution of fossil and non-fossil sources to the ambient PM[19,56,74–78]. The aerosol transformation processes from the original source might lead to isotopic fractionation (kinetic or equilibrium) resulting in a slightly different isotopic composition of the emitted aerosols than its original source[39,43,55,79,80] (Fig. 1). For example, chamber-based experiments by Irei et al. (2006) showed that secondary organic aerosol (SOA) generated by OH-radical reactions with toluene resulted in about 0.6 ± 0.2‰ lower $\delta^{13}C$ value of SOA than the gas phase products. On the other hand, combustion typically results in about 1.3 ± 0.5‰ lower $\delta^{13}C$ in the exhaust gases relative to the liquid fossil fuels whereas $\delta^{13}C$ value does not change during coal burning[38]. During long-range-transport of aerosols, photochemical aging could result in up to 1.5-3‰ enrichment in ^{13}C in remaining aerosols compared to their sources[40,53]. Nevertheless, the final isotopic composition of the sampled aerosol carries information on the primary sources as well as the transformation processes such as secondary formation and aging[47,81–83]. However,

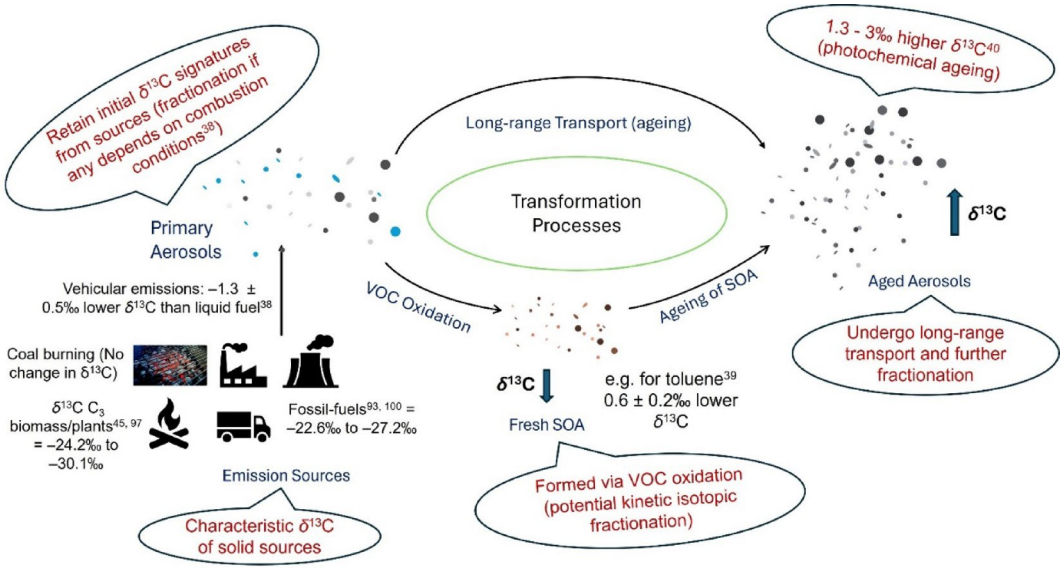

Fig. 1. Schematic showing stable carbon isotopic fractionation and related change in the $\delta^{13}C$ value of aerosols (↑ indicate ^{13}C-enrichment and ↓ indicate ^{13}C-depletion) through various stages of aerosol emission, formation, and atmospheric processing[38–40,45,93,97,100].

the deconvolution of the final isotopic composition of PM to determine the primary sources requires that the isotopic composition of sources must be distinct, and the associated isotopic fractionations are well known.

In this work, we have evaluated the carbon isotopic variability in heavily polluted (urban) and pristine sites (background) in India and assessed the use of $\delta^{13}C$ in characterizing and understanding the origin of carbonaceous aerosols. We determined $\delta^{13}C$ variations in $PM_{2.5}$ aerosols from eight strategic sampling locations of the National Carbonaceous Aerosols Program – CarbOnaceous AerosoL Emissions, Source apportionment & ClimatE Impacts (NCAP-COALESCE) network of the government of India. In this network, the sampling stations have been selected to assess the influence of anthropogenic pollutants, particularly carbonaceous aerosols, on climate change[24]. One of our primary objectives is to evaluate whether $\delta^{13}C$ of aerosols can be used as a standalone proxy for quantitative source apportion estimates so that users are aware of the advantages and pitfalls of this proxy, which has been increasingly utilized in characterizing source signature of CA. The novelty of our study lies in utilizing seasonal $\delta^{13}C$ datasets from multiple sites in India characterized by diverse local climate/environment and the Keeling plot to evaluate the site-specific source dominance.

Procedure and methods

Sampling sites

Eight sampling sites spanning across eight states of India were selected based on different criteria such as emission inventory, wind trajectories, dispersion modeling results, and cross-correlation (r) and coefficient of divergence (COD) analyses. These analyses aided in identifying sampling locations for overall regionally representative aerosols, i.e., without the influence of local pollution sources[84]. The sampling locations are (Fig. 2): Kashmir (KMR, northern Himalayan region in Jammu and Kashmir, 34.13 ^{0}N, 74.84 ^{0}E), Mohali (MOH, upwind Indo-Gangetic Plains in Punjab, 30.67 ^{0}N, 76.73 ^{0}E), Rohtak (RTK, upwind Indo-Gangetic Plains in Haryana, 28.88 ^{0}N, 76.62 ^{0}E), Bikaner (BKN, western arid desert region in Rajasthan (28.03 ^{0}N, 73.26 ^{0}E), Bhopal (BPL, central India in Madhya Pradesh, 23.28 ^{0}N, 77.27 ^{0}E), Shyamnagar (SHY, downwind Indo-Gangetic Plains in West Bengal, 22.50 ^{0}N, 88.23 ^{0}E), Jorhat (JOR, North-East India in Assam, 26.73 ^{0}N, 94.15 ^{0}E), and Mysuru (MYS, background site in southern India in Karnataka, 12.31^{0}N, 76.61 ^{0}E). Figure 2 presents the sampling locations along with population density, and the presence of power plants and cement industries, which are likely sources

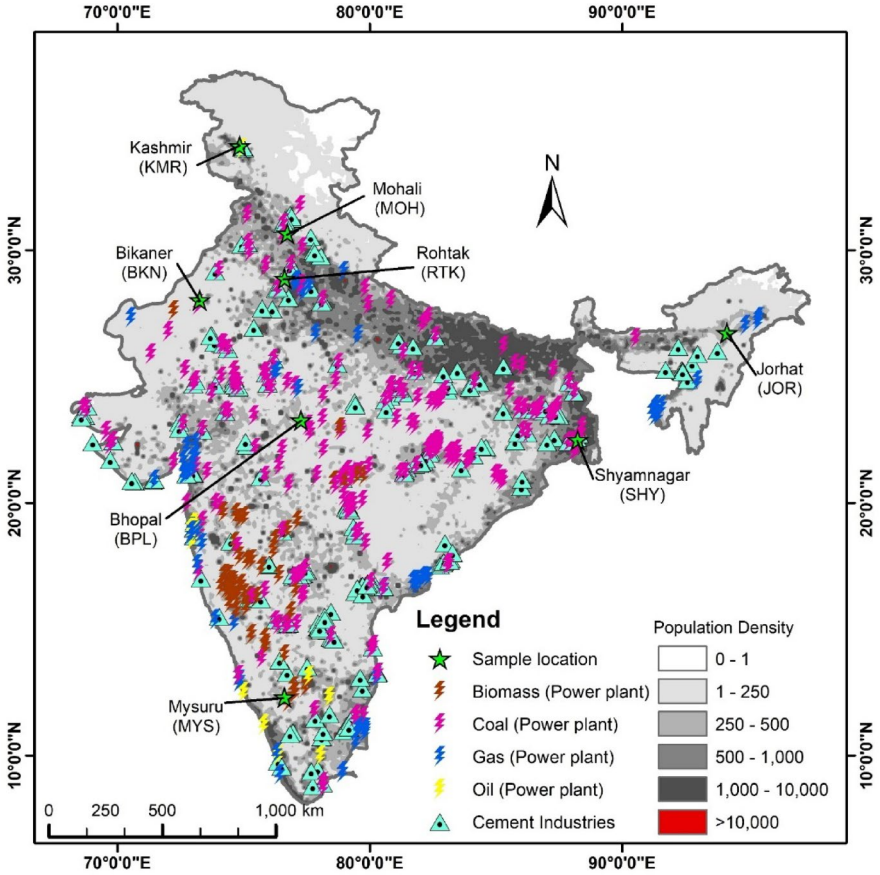

Fig. 2. Map of India showing the NCAP-COALESCE sampling locations (KMR, MOH, RTK, BKN, JOR, BKN, SHY, and MYS). Also shown are the areas likely to have higher anthropogenic emissions of CA, (1) population distribution per square kilometer in greyscale with densely populated regions in red (data from: (1) https://data.worldpop.org/GIS/Population_Density, accessed on January 15, 2025), (2) major powerplants consuming biomass, coal, gas, and oil[114], (3) cement industries[115].

of anthropogenic CA emissions. The KMR sampling site is located at 1500 amsl in a semi-urban setting within the University of Kashmir campus in the Kashmir Himalaya region, characterized by a temperate climate. The MOH sampling site is located in an urban environment within the IISER Mohali campus in the southern part of Chandigarh city in Punjab, north-west India, dominated by monsoonal climate. The BKN sampling site is located within the Maharaja Ganga Singh University campus, which is in the Thar desert region (dry and arid) of Rajasthan in northwestern India. The SHY site was within the Bose Institute campus in Shyamnagar, West Bengal, India, an urban setting with a prevailing humid subtropical climate. The JOR site is located at CSIR-Northeast Institute of Science and Technology, Council of Scientific and Industrial Research (CSIR-NIEST) campus, Assam near the Brahmaputra River in a rural environment. The MYS site is in Karnataka, south-west India, characterized by a tropical savanna climate, and considered a background site due to minimal influence from emission-based sources. The RTK site is in the state of Haryana about 70 km north-west of New Delhi, characterized by a subtropical monsoon climate. The BPL sampling site is within the IISER Bhopal campus, Madhya Pradesh, Central India, having a subtropical climate characterized by hot summer and mild winter.

Sampling details

Aerosol samples ($PM_{2.5}$) were collected on (prebaked at 550 ^{0}C) Quartz-fiber filters (47 mm diameter) from January to December 2019 at eight sampling sites in India on every alternate day. A speciation air sampling system (SASS, Met One Instruments Inc., USA) with five channels was utilized for collecting 24-h time-integrated samples using a mass flow controller unit operated at ~ 6.7 $m^3\ h^{-1}$ flow rate. Every two weeks, field blank samples were also collected to account for sampling artifacts and perform background correction. Sampling details have been provided in previous studies from the NCAP-COALESCE network[85–92].

Analytical procedure

The stable carbon isotopic composition (δ^{13}C value) of aerosols was determined at the stable isotope analytical facility of the Indian Institute of Technology Kanpur (IITK) using an elemental analyzer (Flash EA 2000, Thermo Scientific) coupled with a stable isotope ratio mass spectrometer (IRMS; Thermo Scientific Delta V Plus) in a continuous-flow mode. The detailed analytical procedure was given in our previous studies[45,48,93]. Briefly, about 500–2000 µg of the sample was taken from a quartz filter, packed in air-free tight tin capsules and dropped into an elemental analyzer, resulting in the combustion of the sample and generation of CO_2 in stoichiometrically equivalent amount of carbon present in the sample. The generated CO_2, after online purification and removal of moisture, was transferred to the IRMS via a ConFlow IV interface, and its $^{13}C/^{12}C$ ratio was measured. All isotopic data are represented in δ notation on the VPDB scale (Vienna Pee Dee Belemnite) as:

$$\delta^{13}C_{sample}\,(‰;\ VPDB)\ =\ [\left(^{13}C/^{12}C\right)_{sample}\ /\ \left(^{13}C/^{12}C\right)_{VPDB} - 1]\ x\ 10^3$$

A set of carbon isotope reference standards (LSVEC: -46.6‰; NBS-19: 1.95‰; and IAEA-600: -27.711‰) from the International Atomic Energy Agency (IAEA) were analyzed along with each set of unknown samples to convert raw carbon isotope ratios to the VPDB scale using the normalization procedure described in Paul et al.[94]. Analytical precision based on repeat analyses of a check standard (IAEA-601: -28.81‰) was -28.83 ± 0.04‰ (n = 28). In total 1120 samples have been analyzed along with an additional 32 repeat analyses. The analytical procedure for the measurement of total carbon (TC = OC + EC) is described in the supplementary section.

Spatial distribution maps of δ^{13}C

δ^{13}C values obtained from this study (see Table 1) and reported by others (see Table 2) for different Indian sites were used to create aerosol δ^{13}C spatial variability maps for each season, using GIS technique. Spatial interpolation was performed using the Inverse Distance Weighted (IDW) method available in the Geostatistical Analyst toolbar of ArcGIS®. IDW interpolation, a commonly employed technique for mapping variables, offers an exact and convex method that fits continuous spatial variation models. It relies on distances to weight known locations and uses these values to estimate those at new points[95,96].

	δ^{13}C (‰)			
Location	Winter	Pre-Monsoon	Monsoon	Post-Monsoon
Kashmir (KMR)	-27.6 ± 0.5 **(37)**	-27.2 ± 0.3 **(39)**	-26.8 ± 0.4 **(33)**	-27.7 ± 0.5 **(17)**
Mohali (MOH)	-25.6 ± 0.6 **(34)**	-26.2 ± 0.8 **(30)**	-26.1 ± 0.6 **(36)**	-26.5 ± 0.4 **(23)**
Rohtak (RTK)	-25.9 ± 0.6 **(34)**	-26.4 ± 0.8 **(28)**	-26.4 ± 0.3 **(32)**	-26.8 ± 0.7 **(19)**
Bikaner (BKN)	-26.1 ± 0.4 **(32)**	-25.8 ± 1.0 **(23)**	-25.1 ± 3.2 **(25)**	-26.4 ± 0.5 **(20)**
Bhopal (BPL)	-26.0 ± 0.5 **(46)**	-27.0 ± 0.5 **(46)**	-27.0 ± 0.3 **(44)**	-26.6 ± 0.4 **(30)**
Jorhat (JOR)	-27.7 ± 0.3 **(41)**	-27.2 ± 0.3 **(38)**	-27.3 ± 0.3 **(33)**	-27.5 ± 0.2 **(20)**
Shyamnagar (SHY)	-26.4 ± 0.3 **(45)**	-27.0 ± 0.4 **(44)**	-27.4 ± 0.5 **(60)**	-26.4 ± 0.6 **(28)**
Mysuru (MYS)	-25.5 ± 0.4 **(46)**	-26.2 ± 0.3 **(46)**	-26.8 ± 0.3 **(61)**	-26.1 ± 0.4 **(30)**

Table 1. δ^{13}C values in different seasons at various NCAP locations. *Values in bold represent the number of samples. δ^{13}C (average) ± 1σ for different seasons reported.

$\delta^{13}C$ (‰)	PM size	Location	Type of Site	Reference
−25.6 ± 0.6 (Pre-monsoon)	PM_{10}	Arabian sea	Marine	104
−26.5 ± 0.8 (Pre-monsoon)	PM_{10}	Bay of Bengal	Marine	104
−25.3 ± 0.6 (Winter)	$PM_{2.5}$	Kanpur, India	Urban	93
−25.0 ± 0.6 (Winter and Summer)	PM_{10}	Chennai, India	Urban	117
−27.4 ± 0.5 (Pre-monsoon)	$PM_{2.5}$	Beas, India	Semi-Urban	45
−26.5 ± 0.4 (Post-monsoon)	$PM_{2.5}$	Beas, India		45
−26.4 ± 0.5 (Monsoon)	$PM_{2.5}$	Beas, India		45
−26.5 ± 0.3 (Summer)	PM_{10}	Mumbai, India	Urban	113
−25.9 ± 0.3 (Winter)	PM_{10}	Mumbai, India		113
−24.8 ± 0.9 (Winter)	TSP	Goa, India	Marine	81
−24.9 ± 1.3 (Summer)	TSP	Goa, India		81
−23.9 ± 0.5 (Winter)	TSP	Hisar, India	Urban	41
−24.9 ± 0.6 (Winter)	TSP	Manora Peak, India	Hilly	41
−24.0 ± 0.7 (Winter)	TSP	Arabian Sea	Marine	47
−26.4 (Post-monsoon)	$PM_{2.5}$	Delhi, India	Urban	116
−25.5 (Post-monsoon)	PM_{10}	Delhi, India	Urban	99
−25.4 (Winter)	PM_{10}	Varanasi, India	Urban	99
−26.0 (Winter)	PM_{10}	Kolkata, India	Urban	99
−27.5 (−29.6 to −25.8) (Summer and Monsoon)	PM_{10}	Jodhpur, India	Semi-Urban	98
−28.9 (−31.0 to −27.1) (Summer and Monsoon)	PM_{10}	Ahmedabad, India	Urban	98

Table 2. $\delta^{13}C$ values in different seasons at various sites in India from previous studies. *TSP: Total Suspended Particulate.

Results and discussion

Annual variation of $\delta^{13}C$ at the sampling sites

The $\delta^{13}C$ and TC of $PM_{2.5}$ exhibit significant variability among NCAP-COALESCE sampling sites along with showing seasonal variability at specific sites (Figs. 3 and 4, and S1, Table 1 and Table S1). The highest and lowest $\delta^{13}C$ values of −16.0‰ (14th July 2019) and −29.4‰ (6th September 2019) were recorded at the Bikaner and Shyamnagar sites, having a low TC content of ~ 0.8 μg m^{-3} at both the sites (Fig. 3, Fig. S1). The overall average $\delta^{13}C$ for samples analyzed in this study is −26.6 ± 0.9‰ (1σ). The overall variabilities at individual sites, that is the difference between the maximum and minimum $\delta^{13}C$ values in increasing order are: Jorhat (1.9‰), Mysuru (2.5‰), Kashmir (2.9‰), Bhopal (3.4‰), Rohtak (3.7‰), Mohali (3.8‰), Shyamnagar (4.0‰), and Bikaner (12.2‰). Jorhat (Assam) located in North-East India showed the least variation in $\delta^{13}C$ (< 2‰) among all the sites, whereas Bikaner showed the largest variation of ~ 12‰ (Fig. 4). Barring Kashmir and Jorhat, every other sampling site shows relatively ^{13}C-rich (higher $\delta^{13}C$ values) signature in the winter season (Table 1). Figure 5 shows distinct seasonal $\delta^{13}C$ spatial variability. The overall average TC content in our samples is 14.8 ± 17.4 μg m^{-3}, with the highest TC content of ~ 75 μg m^{-3} in post-monsoon at the RTK site and the lowest value of ~ 1.5 μg m^{-3} in monsoon at BKN and MYS background sites (Table S1). TC contents in our samples strongly correlate with the aerosol mass concentrations. Seasonal variations in the TC content are significant and generally are higher during winter across most sites with RTK and KMR recording elevated levels (Fig. 3b, Fig. S1; Table S1). Interestingly, Rohtak and Mohali located in upwind IGP have significantly higher TC during post-monsoon, which is dominated by biomass burning in this region (Figs. S1 and S2). Monsoon season consistently shows the lowest TC values, likely due to enhanced wet deposition. Site-wise discussion of $\delta^{13}C$ in $PM_{2.5}$ is provided next.

Bhopal

The $\delta^{13}C$ of $PM_{2.5}$ in these samples ranges from −28.1‰ to −24.7‰ (−26.6 ± 0.6‰) (Figs. 3a and 4)[88]. An average $\delta^{13}C$ of ~ −27.0‰ in pre-monsoon and monsoon (Table 1) indicates the contribution of C_3 biomass and/or wood combustion; $\delta^{13}C$ of C_3 plants from India, like globally (−20‰ to −32‰)[97], varies from −24.2‰ to −30.1‰[92]. $\delta^{13}C$ of PM in pre-monsoon and monsoon at Bhopal are similar to those observed in the same seasons at other Indian locations [e.g., Beas (pre-monsoon, $PM_{2.5}$): −27.4 ± 0.5‰[45]; Jodhpur (summer and monsoon, PM_{10}): −27.5‰[98] (Table 2). On the other hand, the $\delta^{13}C$ in the winter season varies from −27.0‰ to −24.7‰ (−26.0 ± 0.5‰). The average $\delta^{13}C$ in winter is very similar to those observed in another IGP location in Kolkata in winter ($\delta^{13}C$ of PM_{10} of −26.0‰[99], Table 2). $\delta^{13}C$ variation in winter at Bhopal suggests an additional contribution from a ^{13}C-rich source, such as the fossil fuel sources including gasoline/diesel/biodiesel vehicular exhaust (−22.6 to −27.2[93,100]). Photochemical aging in aerosols during long-range transport also results in ^{13}C enrichment leading to a higher $\delta^{13}C$ value (up to ~ 3.3‰ for water-soluble organic carbon[52]) in remaining aerosols[47–101]. Yadav et al. (2022)[88] interpreted the isotopic variability in conjunction with the secondary organic carbon (SOC) contributions in both seasons and identified two separate mechanisms. According to them, high SOC/OC ratios in monsoon suggest an influence of SOC formation in the aqueous phase. Through aqueous

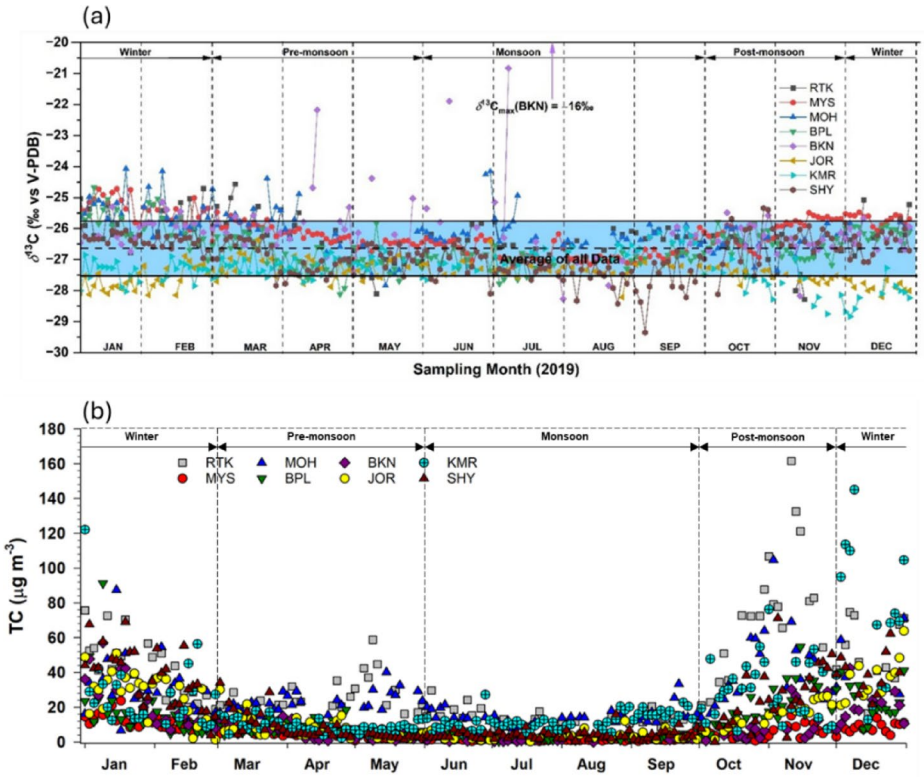

Fig.3. (**a**) Annual variation of $\delta^{13}C$ in carbonaceous ($PM_{2.5}$) aerosols at different NCAP-COALESCE sites. Horizontal dotted line is the average $\delta^{13}C$ and the shaded region (light blue) represents the standard deviation. 3(**b**) Annual variation of TC in $PM_{2.5}$ aerosols at different NCAP-COALESCE sites. RTK: Rohtak; MYS: Mysuru; MOH: Mohali; BPL: Bhopal; BKN: Bikaner; JOR: Jorhat; KMR: Kashmir; SHY: Shyamnagar.

phase chemistry, the highly water-soluble volatile organic compounds (VOCs) are transformed to the particle phase SOC with lower $\delta^{13}C$ than precursors because of kinetic fractionation[39,92,102]. While in post-monsoon and winter, a relative increase in $\delta^{13}C$ of ~ 1‰ (t-test, $p < 0.0001$) relative to the monsoon has been related to the biomass-burning aerosols originating from upwind north-west IGP region dominated by post-harvest biomass burning. However, as discussed before, photochemical oxidation could also lead to this ~ 1‰ enrichment. Therefore, to deduce source characteristics, other parameters should be used together with the $\delta^{13}C$ value.

Bikaner

The $\delta^{13}C$ of Bikaner site varies from −28.3‰ to −16.0‰ (−25.8 ± 1.8‰), indicating contribution from different sources (Table 1; Figs. 3a and 4). The average $\delta^{13}C$ at Bikaner is 1.7‰ higher than that (−27.5‰ in PM_{10}, Table 2) observed at a similar nearby location in Jodhpur, Rajasthan[98]. In this desert region, resuspended dust is a major source of ambient aerosols[103], which is not the case for most of the other Indian locations. As a result, even in the monsoon, it has a characteristic $\delta^{13}C$ signature (−25.1 ± 3.2‰; Table 1) with wide variability, compared to other sites (Figs. 5 and 6). Roy et al. (2023)[103] analyzed the microphysical, optical, and chemical properties of fine aerosol collected from Bikaner City from October 2020 to January 2021, and reported a significant contribution of mineral dust to the ambient aerosol concentrations in this desert region. They reported an 11% contribution of mineral dust to total $PM_{2.5}$ mass, with fine dust concentrations increasing from 9.3 ± 5.6 to 13.6 ± 6.7 μg m^{-3} across clean to high pollution periods, which is not typical in other urban or rural regions. Others have argued that biomass burning is not a significant contributor to ambient pollution in this region but transboundary pollution from biomass burning, dominant in the Punjab and Haryana regions, can have an impact in this region[103].

Jorhat

Jorhat has a typical tropical monsoonal climate characterized by high humidity and heavy rainfall. The $\delta^{13}C$ at the Jorhat (rural) site is homogeneous and varies little from −28.2‰ to −26.4‰ (−27.4 ± 0.3‰, Figs. 3a and 4, Fig. S1), indicating contribution from the same source(s) or different sources with the same composition throughout the year. A slightly higher $\delta^{13}C$ (t-test, $p < 0.0001$) of $PM_{2.5}$ for pre-monsoon (−27.2 ± 0.3‰) and monsoon (−27.3 ± 0.3‰) than winter (−27.7 ± 0.4‰) and post-monsoon (−27.6 ± 0.3‰) is observed (Table 1). $\delta^{13}C$ at Jorhat is much lower compared to other nearby locations of the Bay of Bengal (−26.5 ± 0.8‰ in pre-monsoon PM_{10}) and Kolkata having −26.0‰ in winter PM_{10} (Table 2)[99,104]. Although $\delta^{13}C$ values indicate the source to be dominantly C_3 biomass origin, information on atmospheric processes cannot be deduced solely from this parameter. Qadri et al. (2022)[86] performed cluster analysis and potential source contribution function

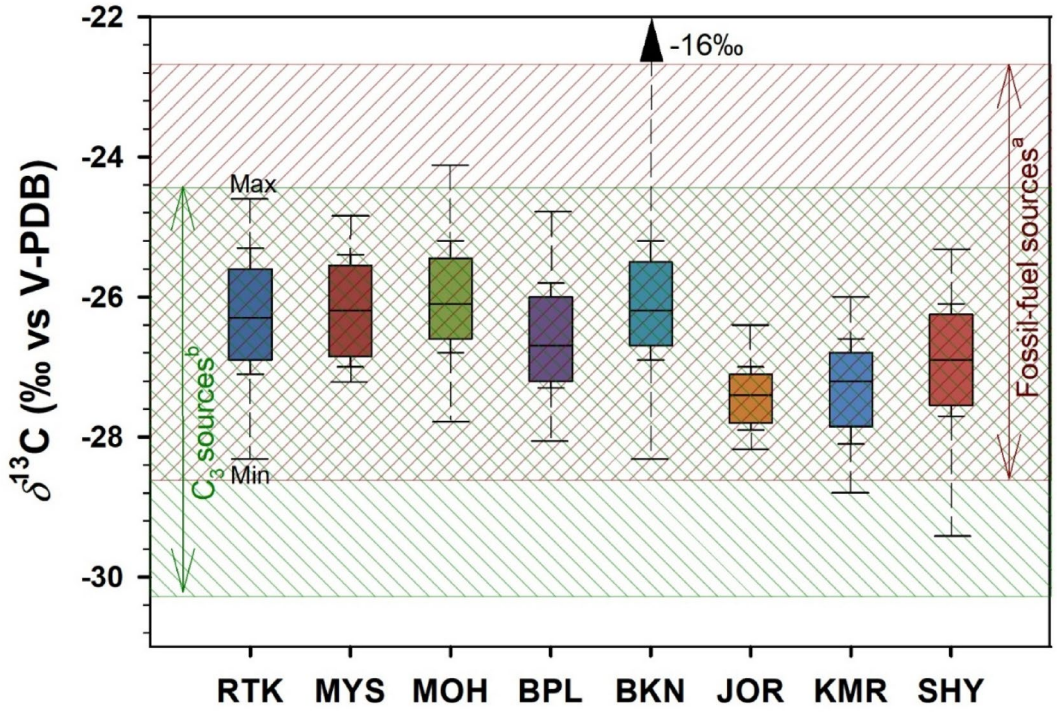

Fig. 4. Plot showing annual median (box plot of variabilities) $\delta^{13}C$ at the NCAP sampling locations along with $\delta^{13}C$ of sources from literature: (**a**) range of fossil fuel combustion from −22.6‰ to −27.2‰[100], and (**b**) C_3 biomass combustion from −24.2‰ to −30.1‰[45,93]. RTK: Rohtak; MYS: Mysuru; MOH: Mohali; BPL: Bhopal; BKN: Bikaner; JOR: Jorhat; KMR: Kashmir; SHY: Shyamnagar.

(PSCF) modeling considering total carbon (TC) in conjunction with $\delta^{13}C$ data and identified C_3 biomass/biofuel combustion to be the primary source of aerosols. Their modeling results also identified that a slightly higher $\delta^{13}C$ during the pre-monsoon (−27.2 ± 0.3‰) and monsoon (−27.3 ± 0.3‰) relative to the winter (−27.7 ± 0.4‰) and post-monsoon (−27.6 ± 0.3‰; Table 1) was due to contribution from aged aerosols and enhanced secondary aerosols derived from photo-oxidation during winter and post-monsoon. Such information cannot be obtained solely from $\delta^{13}C$ of aerosols.

Kashmir

The $\delta^{13}C$ of aerosols ranges from −28.8‰ to −26.0‰ (−27.3 ± 0.5‰, Figs. 3a and 4, Fig. S1), suggesting a minor change in the sources of aerosols. The isotopic compositions strongly suggest a source dominated by C_3 biomass/biofuel combustion and negligible influence of industrial pollution. Whereas the post-monsoon (-27.7 ± 0.5‰), winter (-27.6 ± 0.5‰), and pre-monsoon (-27.2 ± 0.3‰) seasons show similar average $\delta^{13}C$ values, that for the monsoon season is slightly ^{13}C rich (-26.8 ± 0.4‰, t-test, $p < 0.0001$; Table 1). The higher $\delta^{13}C$ in monsoon could be a result of the influence of a low volatile fraction of organic carbon (LVOC) which makes up a refractory fraction of organic carbon due to photochemical processing/oxidation[105]. Qadri et al. (2022)[86] showed that higher LVOC corresponded to higher $\delta^{13}C$, which suggests more influence from aged organic carbon fractions. Lower $\delta^{13}C$ in pre-monsoon at Kashmir is comparable to Beas (-27.4 ± 0.5‰, $PM_{2.5}$)[45] and Jodhpur (-27.5‰, PM_{10}) (Table 2), and could be attributed to enhanced secondary organic aerosol production[45]. The seasonal variation of $\delta^{13}C$ at Kashmir was more or less similar to the Jorhat site located in NE India in a similar Himalayan setting (Fig. 5).

Mohali

$\delta^{13}C$ at the MOH site ranges from −27.8‰ to −24.1‰ (Figs. 3a and 4, Fig. S1). The $\delta^{13}C$ value during the post-monsoon (-26.5 ± 0.4‰) was ~1‰ less than that of the winter season (-25.6 ± 0.6‰) (Table 1). The seasonal (post-monsoon and winter) $\delta^{13}C$ at Mohali was very similar to those observed at other IGP locations such as Beas, Kanpur, Delhi, and Varanasi (Table 2). The winter in this area is significantly dominated by post-harvest open biomass burning (Fig. S2). Using $\delta^{13}C$ of carbonaceous aerosols collected during October 2016 (post-monsoon) and May 2018 (pre-monsoon) from a site in this region (Beas, Punjab) as an input parameter in an isotope mixing model, Singh et al. (2021)[45] concluded that biomass/bio-fuel combustion is a significant source of air pollution in every season in this region. Singh et al. (2021)[45] also utilized organic carbon (OC), elemental carbon (EC) measurements and their sub-fractions such as OC1, OC2, OC3, OC4, EC1, EC2, EC3 of aerosols/sources and air mass back trajectory (AMBT) analysis to strengthen their conclusions. However, fossil fuel-based sources (gasoline: −26.1‰; diesel: −26.3‰; bio-diesel: −26.5‰)[93] contribute more to the pollution episodes during the monsoon and post-monsoonal periods (Fig. 6). $\delta^{13}C$ observed in monsoon (−26.1 ± 0.6‰)

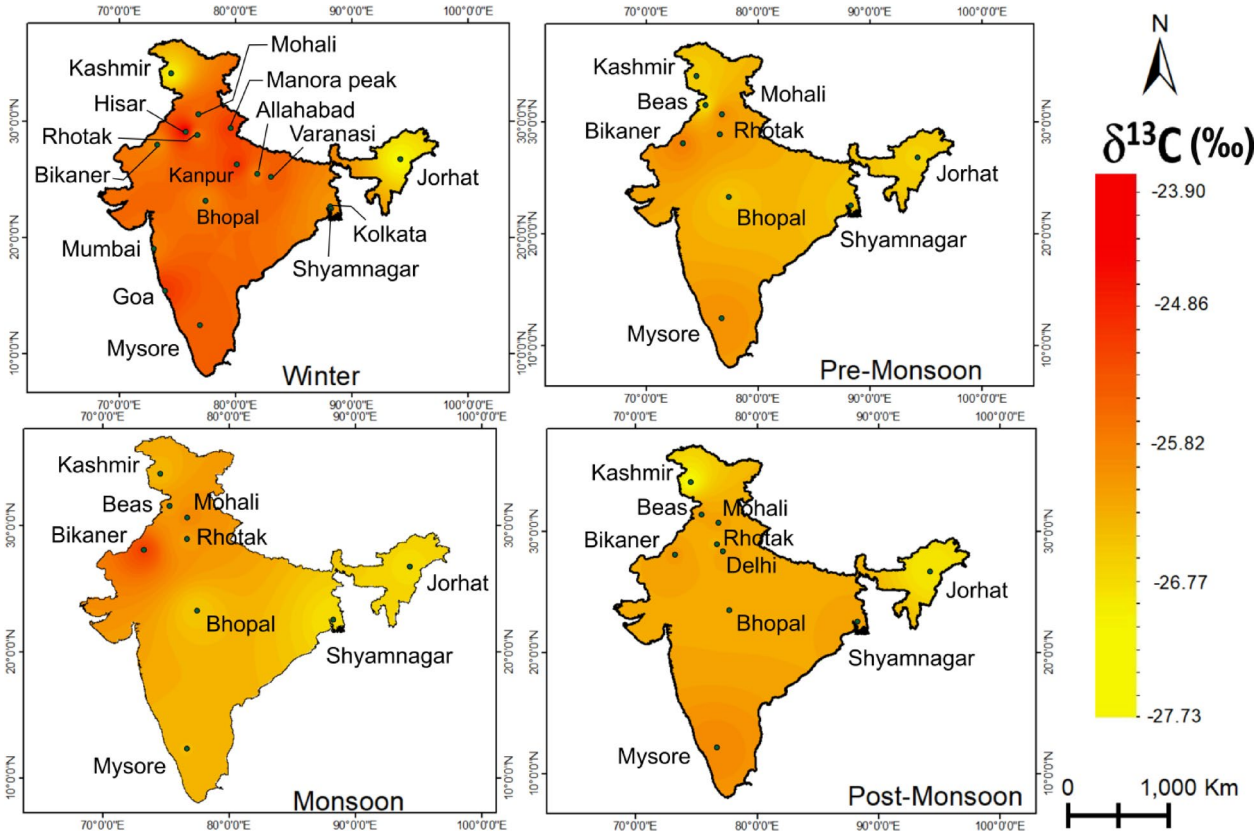

Fig. 5. Spatial distribution map showing $\delta^{13}C$ variability in India in different seasons. Data generated in this study (Table 1) and from the literature (Table 2) were used to prepare these maps.

and post-monsoon (−26.5 ± 0.4‰) in Mohali is similar to that observed in Beas (monsoon: −26.4‰ and post-monsoon: −26.6‰; Table 2)[45]. Moreover, the formation of secondary aerosols through photochemical oxidation (gas-to-particle partitioning) caused during the aging of aerosols results in an enrichment of ^{13}C in the particle phase[47,52]. Such enrichment could explain the ~ 1‰ higher $\delta^{13}C$ values in winter and pre-monsoon compared to that of monsoon and post-monsoon in Mohali (Figs. 4 and 6)[45].

Rohtak

The $\delta^{13}C$ of $PM_{2.5}$ ranged from −28.3‰ to −24.6‰ (Figs. 3a and 4). The $\delta^{13}C$ values of pre-monsoon (−26.4 ± 0.8‰), monsoon (−26.4 ± 0.3‰), and post-monsoon (−26.8 ± 0.7‰) are similar, but the winter season PM was slightly ^{13}C-rich (−25.9‰ ± 0.6‰; Table 2). The seasonal $\delta^{13}C$ was comparable with IGP locations Beas (−26.5 ± 0.4‰ for post-monsoon and −26.4 ± 0.5‰ for Monsoon $PM_{2.5}$), Delhi (−26.4‰ for post-monsoon $PM_{2.5}$), and Kolkata (−26.0‰ for winter PM_{10}) (Table 2). In winter, the $\delta^{13}C$ of $PM_{2.5}$ at Rohtak (−25.9‰) was lower than those observed at a nearby location in Hisar (−23.9 ± 0.5‰[19]; Table 2). In this region, winter, pre-monsoon, and post-monsoon are dominated by post-harvest combustion of paddy and wheat residue (C_3 biomass). These seasons also exhibit an overall $\delta^{13}C$ variability of up to 0.8‰ relative to that of the monsoon season (0.3‰; Table 1). Enriched values in winter could result from aqueous phase processing of aerosols during which the aerosols encounter water droplets in clouds or fog and trigger chemical reactions and transformations[106]. During these interactions, the lighter ^{12}C isotope is typically removed or oxidized more readily, resulting in enrichment in ^{13}C (higher $\delta^{13}C$) in the remaining aerosols[80]. Using the United States Environmental Protection Agency's IsoSource linear mixing model, Singh et al.[45] inferred significant influence from fossil fuel-based vehicular sources in this region (gasoline: −26.1‰; diesel: −26.3‰; bio-diesel; −26.5‰) during pre-monsoon and monsoon.

Mysuru

The annual $\delta^{13}C$ in Mysuru varied between −27.2‰ to −24.7‰ (Figs. 3a and 4, Fig. S1). The $\delta^{13}C$ in winter (-25.5 ± 0.4‰) was ~ 1‰ enriched in ^{13}C compared to other seasons (pre-monsoon, monsoon, and post-monsoon: average $\delta^{13}C$ of −26.4 ± 0.5‰) (Table 1). Yadav et al. (2022)[88] utilized $\delta^{13}C$ along with OC, EC, and water-soluble inorganic ions in the aerosols and argued that proximal vehicular exhaust emissions contributed carbonaceous aerosols during pre-monsoon, monsoon, and post-monsoon. The variation of $\delta^{13}C$ in winter was between −26.1‰ to −24.5‰ and when plotted against the reciprocal of $PM_{2.5}$ mass concentration (Keeling Plot)[107], indicated contributions from traffic (petrol and diesel) and coal-based combustion sources (see Fig. 2 of Yadav et al.[88]). This conclusion was also supported by a MixSIAR model (Bayesian mixing model) derived proportional contribution of 71% from fossil-based sources.

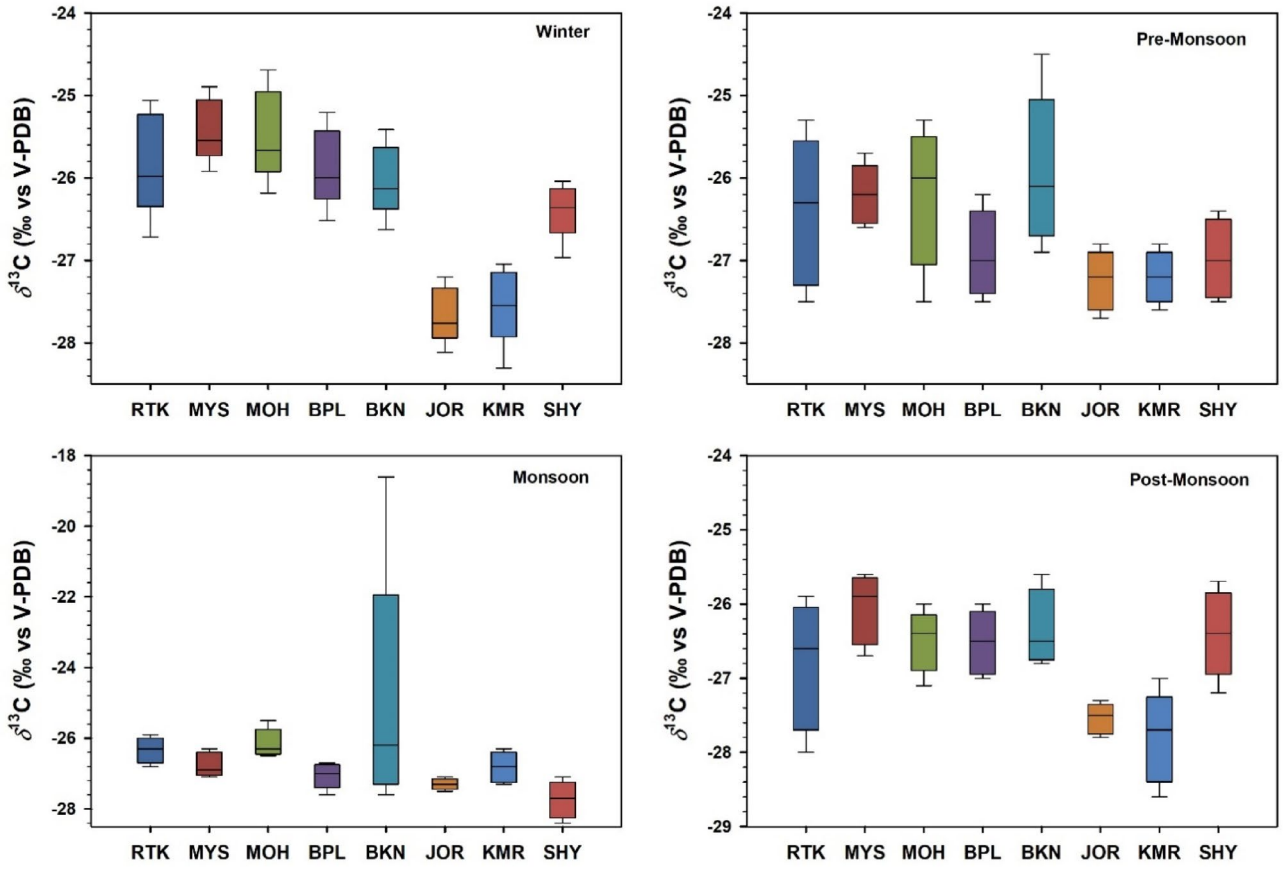

Fig. 6. Box plot depicting seasonal variabilities in $\delta^{13}C$ at eight NCAP sites.

Shyamnagar

The $\delta^{13}C$ of $PM_{2.5}$ at SHY varied between −29.3‰ to −25.3‰ (Figs. 3a and 4, Fig. S1). Wintertime average $\delta^{13}C$ at Shyamnagar was −26.4 ± 0.3‰ and post-monsoon average was −26.4 ± 0.5‰, which was marginally higher than pre-monsoon and monsoon averages of −27.0 ± 0.4‰ and −27.4 ± 0.4‰, respectively (Table 1). $\delta^{13}C$ in winter at Shyamnagar is similar to the neighboring Kolkata (−26.0‰, PM_{10}), as observed in a previous study[99] (Table 2). The $\delta^{13}C$ in pre-monsoon is slightly lower than that observed in the Bay of Bengal (−26.5 ± 0.8‰) reported by Agnihotri et al. (2011)[104]. Utilizing $\delta^{13}C$ versus 1/TC relationship (Keeling plot) in the aerosols from this sampling site, Singh et al. (2023)[92] identified a significant contribution from vehicular exhaust in the post-monsoon and winter seasons, which have nearly similar $\delta^{13}C$ values (− 26.4‰). Also, the results of air trajectory and PSCF analyses suggested that the atmospheric aging of anthropogenic aerosols arriving from upwind IGP could be responsible for the relatively ^{13}C-rich values observed in the winter and post-monsoon seasons. In contrast to winter and post-monsoon, most samples from the pre-monsoon and monsoon were ^{13}C-depleted (about − 1‰ lower) and had the lowest average TC contents of ~ 4 to 8 μg m^{-3} (Fig. S1; Table S1). Singh et al.[92] argued that the influence of SOC (38-72%) in winter and post-monsoon resulted in ^{13}C enrichment, compared to pre-monsoon and monsoon. As an IGP outflow site, Shyamnagar receives aerosols from upwind IGP regions with significant anthropogenic sources during the winter and post-monsoon.

Comparison with $\delta^{13}C$ of aerosols at other sites globally

The average seasonal $\delta^{13}C$ values of carbonaceous aerosols measured at Indian NCAP sites range from -27.7‰ to -25.1‰ and exhibit spatial and seasonal variability (Table 1). We have compared our data (average isotopic compositions) with those from other global sites representing rural/forest, urban, and marine environments, presented in Table 3. Isotopic variability in our sites broadly aligns with global observations, that is higher $\delta^{13}C$ values (^{13}C-enriched signature) are typical of urban and combustion-dominated regions, whereas forest and marine environments are characterized with ^{13}C-depleted signature (lower $\delta^{13}C$ values), excluding the marine site in Okinawa, Japan[119]. For instance, Indian locations like MYS, KMR, and JOR (-26 to -27.7‰), located in less polluted regions, exhibit $\delta^{13}C$ values similar to those in the Arctic Ocean (-27.4 ± 1.3‰) and forest and marine sites in Lithuania (-27.2 to -27.9‰) during summer time (Table 3), indicative of biogenic carbon (C_3 plants) sources. In contrast, urban sites such as MOH and RTK are relatively ^{13}C-enriched (up to -25.5‰), which is comparable to urban settings like Mexico City (-25.4 ± 1.2‰), Prague (-25.5 to -27.2‰), and urban centers in Poland (-25.3 to -26.7‰) and Beijing, China (-23.8 to -24.9‰), highlighting contributions from fossil fuels and vehicular emissions. Interestingly, the isotopic composition of Indian sites is more homogenous

$\delta^{13}C$ (‰)	PM size	Location	Type of Site	Reference
−27.4 ± 1.3 (Summer)	TSP	Arctic Ocean	Marine	111
−26.6 ± 0.8 (Summer)	TSP	Bering Sea	Marine	111
−25.6 ± 2.1 (Summer)	TSP	Northwest Pacific	Marine	111
−25.4 ± 1.2	$PM_{2.5}$	Mexico City, Mexico	Urban	118
−22.5 ± 0.6 (Winter)	TSP	Okinawa, Japan	Marine	119
−22.5 ± 0.7 (Spring)	TSP	Okinawa, Japan		119
−22.9 ± 0.7 (Summer)	TSP	Okinawa, Japan		119
−22.3 ± 0.9 (Autumn)	TSP	Okinawa, Japan		119
−27.6 ± 0.8 (Summer)	PM_1	Vilnius, Lithuania	Urban	105
−27.2 ± 0.2 (Summer)	PM_1	Preila, Lithuania	Marine	105
−27.9 ± 0.5 (Summer)	PM_1	Rugsteliski, Lithuania	Forest	105
−26.6 ± 0.4 (Spring)	$PM_{2.5}$	Prague, Czech Republic	Urban	83
−27.2 ± 0.5 (Summer)	$PM_{2.5}$	Prague, Czech Republic		83
−26.1 ± 0.7 (Autumn)	$PM_{2.5}$	Prague, Czech Republic		83
−25.5 ± 0.8 (Winter)	$PM_{2.5}$	Prague, Czech Republic		83
−24.9 ± 0.2 (Summer)	$PM_{2.5}$	Beijing, China	Urban	76
−23.8 ± 0.2 (Winter)	$PM_{2.5}$	Beijing, China		76
−23.6 ± 1.2 (Summer)	$PM_{2.5}$	Morogoro, Tanzania	Rural	67
−25.3 ± 0.9 (Annual average)	TSP	Montreal, Canada	Various	60
−24.4 to −22.7 (Annual)	TSP	Gosan, South Korea	Marine	53
−26.2 (Winter)	$PM_{2.5}$	Hong Kong	Urban	51
−26.4 (Winter)	$PM_{2.5}$	Hong Kong	Urban	51
−27.0 ± 1.0 (Annual average)	PM_{10}	Zgorzelec, Poland	Urban	44
−25.3 ± 0.9 (Annual average)	PM_{10}	Nowa Ruda, Poland	Urban	44
−26.9 ± 0.7 (Annual average)	PM_{10}	Polkowice, Poland	Urban	44
−26.7 ± 0.9 (Annual average)	PM_{10}	Legnica, Poland	Urban	44
−26.5 ± 1.1 (Annual average)	PM_{10}	Świdnica, Poland	Urban	44

Table 3. $\delta^{13}C$ values of aerosols at selected sites globally, representing urban, rural, and marine locations.

compared to those of the global sites that show a few sites having more ^{13}C-rich signatures (e.g., -22.3‰ at Okinawa, Japan, Table 3). We would like to note that $\delta^{13}C$ variability of aerosols at a specific site is largely controlled by the regional/local combustion sources and anthropogenic emissions, with urban sites showing strong influence from fossil fuel emissions/biomass burning, whereas background and remote sites are more influenced by biogenic or long-range transported carbon.

Seasonality of $\delta^{13}C$ variability at NCAP locations

Winter

Our data show seasonal $\delta^{13}C$ variations at all the sampling sites (Figs. 5 and 6), which can be attributed to a plethora of factors such as the variation of the sources, meteorology and related atmospheric chemistry (Fig. 1). The special distribution map of isotopic variability shows that Kashmir (KMR) and Jorhat (JOR) sites, located in the North and North-East India in the Himalayan foothills, have the lowest average $\delta^{13}C$ values (by 2 to 3‰) compared to other sites during the winter season (Fig. 5). Temperature in winter season in the North and North-East India, especially in the Himalayan regions, becomes much lower compared to other parts of the country. Low rainfall, low wind speed, and low boundary layer height create stagnant conditions in this region. Thus, the particles emitted from the sources do not undergo significant dilution/dispersion and are minimally affected by transformation processes during travel by air masses. Therefore, $\delta^{13}C$ of $PM_{2.5}$ [−27.6 ± 0.5‰ (KMR) and −27.7 ± 0.3‰ (JOR); Table 1] likely represents the composition of its source, which are dominantly C_3 biofuel/biomass or fossil fuel-based sources. The TC contents at KMR and JOR attain the highest values in winter (Table S1). These two locations are also relatively less urbanized and therefore the contribution from other anthropogenic activities such as vehicular/industrial sources are negligible. On the other hand, other Indian locations (RTK, MYS, MOH, BPL, BKN, SHY) show higher $\delta^{13}C$ values in winter (Figs. 5 and 6, and S1), which could be due to the presence of ^{13}C-enriched emission sources and/or aging of particles/SOA formation during transport that could result in ^{13}C enrichment. Chamber-based experiments have demonstrated ~ 2–3‰ ^{13}C enrichment in oxalic acid (a dominant organic aerosol species) through photocatalytic reactions in the aqueous phase[101]. The usual sources of oxalic acid in aerosols could be from direct emissions such as burning biomass and fossil fuels, or secondary production during oxidation of organic precursors such as VOCs. The VOCs, NO_x, and oxidants predominantly originate from vehicular emissions. Aided by unstable air circulation patterns such as turbulence and inversions, these NO_x and VOC precursors could promote secondary production of oxalic acid in urban and polluted areas. These locations are also more urbanized and populated compared to Jorhat and Kashmir with more influence from anthropogenic sources.

Pre-monsoon

The average $\delta^{13}C$ in pre-monsoon exhibits relatively lower values and more overall variability at all locations (except KMR and JOR), compared to the winter season (Figs. 5 and 6). In pre-monsoon, an increase in temperature and sunlight intensity, along with changes in wind speed/direction, results in strong convective mixing of airmasses, causing dispersion of pollutants. Atmospheric processes could result in an increase in $\delta^{13}C$ of aerosols undergoing photochemical aging during long-range transport[47,80]. On the other hand, enhanced SOA formation due to photochemical oxidation in pre-monsoon/summertime would result in ^{13}C depletion in the oxidation products and ^{13}C enrichment in the precursors (Fig. 1). Kashmir (KMR) in the Upper Himalayan Region and Jorhat (JOR) in the foothills of lower Himalaya exhibited an increase in $\delta^{13}C$ in pre-monsoon compared to the winter season (Fig. 6). It has been observed that the products in the aerosol phase are more enriched in ^{13}C than in the gaseous phase if equilibrium separation between phases takes place[79]. It is possible that $PM_{2.5}$ in KMR and JOR undergoes a transformation process due to unique atmospheric conditions in which equilibrium fractionation results in ^{13}C enrichment of the product phase. In Kashmir, cooler temperatures enhance the condensation of semi-volatile organic compounds (SVOCs) onto aerosols, enriching heavier isotopes (^{13}C) in the particle phase due to partitioning. In Jorhat, high humidity from rising temperatures and pre-monsoon rains might promote aqueous-phase reactions in droplets, where equilibrium effects preferentially incorporate lighter isotopes (^{12}C) into the liquid phase, leaving particles enriched in ^{13}C (higher $\delta^{13}C$). These contrasting conditions may amplify isotopic enrichment at these locations compared to other locations.

Monsoon

The $\delta^{13}C$ variability (average: -26.6 ± 1.2‰) in monsoon, considering all studied locations, shows an interesting result. The average $\delta^{13}C$ and the magnitude of variability for each location is typically the lowest amongst all seasons, except for the BKN location (Figs. 6). The most ^{13}C-depleted signature of monsoon aerosols could be attributed to the frequent removal of emitted aerosols from the ambient air due to washout/scavenging by rainfall and high humidity, resulting in a signature representative of the isotopic composition of their primary sources. The frequent washout of the aerosols nullifies the isotope fractionation effect of the long-range transport of aerosols and SOA formation. However, $\delta^{13}C$ of BKN shows the largest variability ranging from −16‰ to −28‰ (Figs. 3 and 6), has a more ^{13}C-rich signature (average $\delta^{13}C$ of − 25.1), and is seen as a distinct hotspot in Fig. 5. We attribute this distinct signature to additional influence from marine aerosols. Sudheer et al. (2016)[98] reported $\delta^{13}C$ (av. -27.5‰: -29.6‰ to -25.8‰) of PM_{10} carbonaceous aerosol collected during summer and monsoonal season (May-September) from Jodhpur, located ~ 240 km south of our site BKN. Based on $\delta^{13}C$ and other chemical proxies (WSOC, OC, EC, and ionic species), Sudheer et al.[98] identified a major contribution from biogenic primary emissions and minimal contribution from combustion emissions, SOA formation, or resuspended soil dust and long-range transport. According to Ceburnis et al.[108], the $\delta^{13}C$ of marine aerosols varies from −20.3‰ to −25.3‰. Bikkina et al.[47] reported $\delta^{13}C$ in total suspended particulates (TSP) sampled over the Arabian Sea in winter, from -25.1‰ to -22.9‰. Kirillova et al.[40] showed that the marine aerosols reaching Sinhagad, India (near the west coast) during monsoon were about 2‰ ^{13}C-enriched compared to that of TOC. It is possible that the distinct ^{13}C-rich signature at BKN during monsoon could be influenced by contributions from marine aerosols. However, further tracer studies (such as sodium, chloride, magnesium, calcium ions, and methanesulfonic acid (MSA)) are needed to decipher the quantitative mass contribution of various sources.

Post-monsoon

The $\delta^{13}C$ values during post-monsoon become slightly higher compared to the monsoon and resemble the signature observed for pre-monsoon (Figs. 5 and 6; Table 1). The JOR and KMR sites show lower $\delta^{13}C$ values (average of -27.7‰) relative to the other locations. Fire maps for different seasons during our sampling duration show most fire events originating in the upwind IGP region (Fig. S2), which is related to large-scale post-harvest open biomass (paddy; primarily of C_3 origin) burning in the post-monsoon. A decrease in temperature and boundary layer height (particularly at nighttime) in North India in the post-monsoon results in a stagnant condition[45]. The longer time spent by the particles in these conditions and the associated equilibrium isotopic fractionation between gas and particle result in ^{13}C enrichment in the product aerosols[45]. These conditions are amplified in the winter seasons at most locations causing higher $\delta^{13}C$ in aerosols, distinctly observed in Fig. 5. Further, the WSOC fraction tends to increase the $\delta^{13}C$ of the total carbon which further increases during long-range transport[40,49,80,105], and likely play a major role during post-monsoon and winter in transporting aerosols originating from upwind IGP to Bay of Bengal (BOB) region, which explains relatively higher $\delta^{13}C$ values in winter and post-monsoon aerosols from our study sites.

Use of stable carbon isotope ratios of CA as a stand-alone proxy for source characterization

$\delta^{13}C$ is a valuable tool for investigating several aspects related to the sources of carbonaceous aerosols, but our analysis of data from eight Indian sites implies that its utilization as a standalone proxy for source apportionment purposes has certain limitations. The uncertainty in the source apportionment can arise due to the large range of $\delta^{13}C$ values of sources, causing overlapping isotopic signatures observed for biomass burning, fossil fuels, dust, or industrial sources. For example, Fig. 4 shows that there could be several sources (e.g. C_3 plants and fossil fuels) having overlapping $\delta^{13}C$ values dominating the pollution at a particular location. The isotopic composition of all probable sources, locally or regionally, should be determined to identify characteristic (distinct vs. overlapping) source signatures. Moreover, the degree of atmospheric processing and the isotopic fractionation incurred during transport along with the mixing of multiple sources also complicates the quantification of primary sources (Fig. 1). Atmospheric transformation processes such as different SOA formation mechanisms (photochemical oxidation) depend on the availability of precursors, oxidants, temperature, humidity, and atmospheric stability,

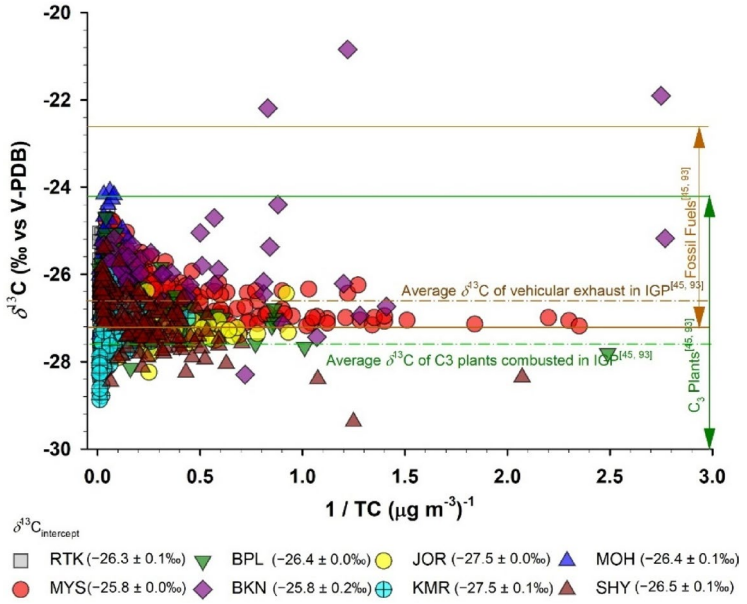

Fig. 7. $\delta^{13}C$ vs. 1/TC of $PM_{2.5}$ aerosols at our NCAP sites. Dashed lines and solid lines indicate average and range of $\delta^{13}C$ of various sources. See Fig. S3 for individual plots.

etc., often characteristics of a specific location[49,80]. The principal factor controlling the initial isotope fractionation is the kinetic isotope effect (KIE), which primarily arises during unidirectional (irreversible) reactions of organic substances[83]. Depending on the KIE, the reaction products may go through additional reactions that result in additional stepwise $\delta^{13}C$ changes, and therefore knowledge of the reaction mechanism and the associated KIE must be known to deduce the primary isotopic composition of the sources.

Nevertheless, $\delta^{13}C$ could be used in conjunction with other chemical tracers such as temperature-resolved carbon fractions OC/EC, WSOC, water-soluble ions (e.g. K^+_{BB}), organic compounds (e.g. levoglucosan), and $\Delta^{14}C$ values to identify and quantify aerosol sources, particularly, identify combustion sources and secondary sources (OC/EC), the contribution of WSOC, proportion of biogenic vs. fossil-derived carbon (using $\Delta^{14}C$ values) and identify biomass burning sources (K^+_{BB}).

For example, others have used $\delta^{13}C$ versus 1/TC (the so-called Keeling plot) for source characterization. The y-intercept of the linear regression in a Keeling plot represents the isotopic signature of the dominant source[107]. The $\delta^{13}C$ versus 1/TC variations in our data and the y-intercepts for our studied sites are given in Fig. 7. The $\delta^{13}C_{intercept}$ for BPL (−26.4 ± 0.0‰) indicates a major contribution from vehicular exhaust[88]. $\delta^{13}C_{intercept}$ for BKN (−25.8 ± 0.2‰) indicate more ^{13}C-enriched sources dominating this site. A few higher 1/TC values at this site indicate low aerosol concentrations and are more ^{13}C-rich (~ −21‰). As discussed before in the previous section and supported by previous studies[40,47,108], this ^{13}C-rich signature at BKN is attributed to contributions from marine aerosols. $\delta^{13}C_{intercept}$ for MYS (− 25.8‰) is also lower with the lowest overall TC content and indicates contributions from traffic (petrol and diesel) and fossil fuel combustion sources[88]. At the Mysuru site, periods with elevated 1/TC values (> 1, Fig. 7) indicate that $\delta^{13}C$ is predominantly influenced by contributions from vehicular exhaust, reflecting the dominance of local combustion-related emissions. Sites JOR (rural) and KMR (semi-urban Himalayan region) exhibit the lowest $\delta^{13}C_{intercept}$ of −27.5‰, suggesting a dominant contribution from C_3 biomass combustion (e.g., wood, crop residue) and less fossil fuel influence. TC values in these regions during the winter are among the highest, consistent with seasonal wood combustion for heating and cooking (Fig. 3b; Table S2). Sites MOH, RTK (and SHY) show similar $\delta^{13}C$ signatures ($\delta^{13}C_{intercept} \approx$ -26.4‰), suggesting contributions from vehicular emissions and C_3 plant combustion, especially during post-harvest seasons.

Air Mass Back Trajectories (AMBTS) can also be used in tandem with $\delta^{13}C$ data for identification of the geographical origin of long- and short-range sources[19,56,92]. Similarly, analyzing forest fire data (e.g., MODIS data) in the region, and identifying fire hotspots could help interpret the carbon isotope composition of aerosols (e.g., Qadri et al.,[86]). Moreover, for improving the accuracy of source apportionments, isotope mixing statistical models such as IsoSource, MixSIAR, and PMF can be utilized alongside other indicators such as OC/EC, ionic species, and metals[56,109–112]. Therefore, correlations between $\delta^{13}C$ and other proxies discussed above, or using these as input parameters in statistical models would reduce the uncertainties in isotopic end member values and improve the model resolution, giving a robust and comprehensive source apportionment of carbonaceous aerosols.

Conclusion

Determination of stable carbon isotope ($\delta^{13}C$) measurements is an advanced analytical technique that is utilized for deciphering the ambient pollution sources and understanding particle formation and transformation processes of carbonaceous aerosols. This work utilizes $\delta^{13}C$ variability in carbonaceous aerosols sampled in a

nationwide NCAP-COALESCE network in India and discusses how good a tracer $\delta^{13}C$ value of aerosols is in tracing (and quantifying) the emission sources. Our data show a distinct $\delta^{13}C$ variability in Indian aerosols both in space and time (seasonal). Out of the eight locations continuously monitored, Jorhat (northeast India) and Kashmir (northern Himalayan region) sites exhibit the most depleted $\delta^{13}C$ values during all seasons. Mohali and Rohtak, located in the upwind IGP, showed similar variations in $\delta^{13}C$ in all four seasons, indicating the dominance of similar sources and atmospheric processes. On the other hand, the Bikaner (arid and dry) site shows more positive $\delta^{13}C$ values during pre-monsoon and monsoon, depicting the influence of resuspended dust (due to high wind speed). In winter and post-monsoon, the $\delta^{13}C$ (at Shyamnagar, Bhopal, and Rohtak) shows the influence of transboundary pollution from other states. Background site Mysuru (southern India) showed more positive $\delta^{13}C$ in winter and post-monsoon season compared to other sites, suggesting the influence of aerosol aging. While other seasons suggested an influence from more negative biogenic sources. Using the y-intercept in a $\delta^{13}C$ versus 1/TC relationship (Keeling plot), we assessed the dominant sources across our study sites. These results indicate that emissions from vehicles/fossil fuels dominate at BPL and MYS sites, whereas C_3 biomass combustion dominates at rural and semi-urban locations like JOR and KMR. On the other hand, MOH, RTK, and SHY locations are influenced by multiple sources, such as post-harvest biomass burning and vehicular combustion. Due to the complex and varied nature of aerosol sources and the potential for isotopic fractionation involved during aerosol formation/transport, $\delta^{13}C$ is not an ideal standalone proxy for source apportionment of atmospheric aerosols. Further, the interpretation of $\delta^{13}C$ can be difficult if sources have overlapping isotopic compositions. However, $\delta^{13}C$ could be used with other proxies such as radiocarbon ($\Delta^{14}C$), OC/EC, K^+_{BB}, AMBTs, trace elements/organic species, and aerosol size distribution, etc., to differentiate between fossil and biogenic sources and perform robust source apportionment estimates. Specific biomarkers like levoglucosan can also be utilized with $\delta^{13}C$ to identify contributions from biomass burning. Isotope mixing statistical models that combine relevant proxies and $\delta^{13}C$ can provide a more accurate estimate of sources and a comprehensive understanding of aerosol composition, their environmental impacts, and climate change.

Data availability

The datasets used and/or analysed during the current study available from the corresponding author on reasonable request. For data, please contact: dapul@iitk.ac.in.

Received: 9 March 2025; Accepted: 23 May 2025
Published online: 04 June 2025

References

1. Kelly, F. J. & Fussell, J. C. Air pollution and public health: emerging hazards and improved Understanding of risk. *Environ. Geochem. Health*. **37**, 631–649 (2015).
2. Bourdrel, T., Bind, M. A., Béjot, Y., Morel, O. & Argacha, J. F. Cardiovascular effects of air pollution. *Arch. Cardiovasc. Dis.* **110**, 634–642 (2017).
3. Ramanathan, V. & Carmichael, G. Global and regional climate changes due to black carbon. *Nat. Geosci.* **1**, 221 (2008).
4. Rajeev, P., Rajput, P., Singh, A. K. & Gupta, T. Study of Temporal variability and mass closure of PM2.5 and its chemical constituents during weak south-west monsoon. *Atmos. Pollut Res.* **9**, 864–870 (2018).
5. Rajeev, P., Singh, A. K., Singh, G. K., Vaishya, R. C. & Gupta, T. Chemical characterization, source identification and health risk assessment of polycyclic aromatic hydrocarbons in ambient particulate matter over central Indo-Gangetic plain. *Urban Clim.* **35**, 100755 (2021).
6. Manisalidis, I., Stavropoulou, E., Stavropoulos, A. & Bezirtzoglou, E. Environmental and health impacts of air pollution: a review. *Front. Public. Health*. **8**, 505570 (2020).
7. Gupta, T., Rajeev, P. & Rajput, R. Emerging major role of organic aerosols in explaining the occurrence, frequency, and magnitude of haze and fog episodes during wintertime in the Indo-Gangetic plain. *ACS Omega*. **7**, 1575–1584 (2022).
8. Jacobson, M. Z. Strong radiative heating due to the mixing state of black carbon in atmospheric aerosols. *Nature* **409**, 695 (2001).
9. Bond, T. C. et al. Bounding the role of black carbon in the climate system: A scientific assessment. *J. Geophys. Res. Atmos.* **118**, 5380–5552 (2013).
10. Velali, E. et al. Redox activity and in vitro bioactivity of the water-soluble fraction of urban particulate matter in relation to particle size and chemical composition. *Environ. Pollut.* **208**, 774–786 (2016).
11. Chirizzi, D. et al. Influence of saharan dust outbreaks and carbon content on oxidative potential of water-soluble fractions of PM2.5 and PM10. *Atmos. Environ.* **163**, 1–8 (2017).
12. Li, S., Zhang, H., Wang, Z. & Chen, Y. Advances in the research on brown carbon aerosols: its concentrations, radiative forcing, and effects on climate. *Aerosol Air Qual. Res.* **23**, 220336 (2023).
13. Contini, D., Vecchi, R. & Viana, M. Carbonaceous aerosols in the atmosphere. *Atmosphere* **9**, 181 (2018).
14. Andreae, M. O. & Gelencsér, A. Black carbon or brown carbon? The nature of light-absorbing carbonaceous aerosols. *Atmos. Chem. Phys.* **6**, 3131–3148 (2006).
15. Zhang, Q. et al. Ubiquity and dominance of oxygenated species in organic aerosols in anthropogenically-influenced Northern hemisphere midlatitudes. *Geophys. Res. Lett.* **34**, L13801 (2007).
16. Moosmüller, H. & Arnott, W. P. Aerosol light absorption and its measurement: A review. *J. Quant. Spectrosc. Radiat. Transf.* **110**, 844–878 (2009).
17. Lelieveld, J., Evans, J. S., Fnais, M., Giannadaki, D. & Pozzer, A. The contribution of outdoor air pollution sources to premature mortality on a global scale. *Nature* **525**, 367–371 (2015).
18. Venkataraman, C., Habib, G., Eiguren-Fernandez, A., Miguel, A. H. & Friedlander, S. K. Residential biofuels in South Asia: carbonaceous aerosol emissions and climate impacts. *Science* **307**, 1454–1456 (2005).
19. Bikkina, S., Kawamura, K. & Sarin, M. Stable carbon and nitrogen isotopic composition of fine mode aerosols (PM2.5) over the Bay of Bengal: impact of continental sources. *Tellus B Chem. Phys. Meteorol.* **68**, 31518 (2016).
20. Fang, W. et al. Divergent evolution of carbonaceous aerosols during dispersal of East Asian haze. *Sci. Rep.* **7**, 10422 (2017).
21. Ramachandran, S. & Rupakheti, M. Year-round aerosol characteristics and radiative effects in the South Asian pollution outflow over a background site in the Maldives. *Atmos. Environ.* **240**, 117813 (2020).
22. Chavan, P. et al. The outflow of Asian biomass burning carbonaceous aerosol into the upper troposphere and lower stratosphere in spring: radiative effects seen in a global model. *Atmos. Chem. Phys.* **21**, 14371–14384 (2021).
23. Sahu, S. K., Beig, G. & Sharma, C. Decadal growth of black carbon emissions in India. *Geophys. Res. Lett.* **35**, L02807 (2008).

24. Venkataraman, C. et al. Indian network project on carbonaceous aerosol emissions, source apportionment and climate impacts (COALESCE). *Bull. Am. Meteorol. Soc.* **101**, E1052–E1068 (2020).
25. Sharma, S., Chandra, M. & Kota, S. H. Four year long simulation of carbonaceous aerosols in India: seasonality, sources and associated health effects. *Environ. Res.* **213**, 113676 (2022).
26. Ramanathan, V. et al. Warming trends in Asia amplified by brown cloud solar absorption. *Nature* **448**, 575–578 (2007).
27. Ram, K., Sarin, M. M. & Hegde, P. Long-term record of aerosol optical properties and chemical composition from a high-altitude site (Manora Peak) in central himalaya. *Atmos. Environ.* **45**, 4233–4242 (2011).
28. Tiwari, S., Dumka, U. C. & Kaskaoutis, D. G. Aerosol physical and optical properties over the Indo-Gangetic plain: implications of aerosol types. *Environ. Sci. Pollut Res.* **24**, 23872–23888 (2017).
29. Laskin, A., Laskin, J. & Nizkorodov, S. A. Chemistry of atmospheric brown carbon. *Chem. Rev.* **115**, 4335–4382 (2015).
30. Shamjad, P. M., Satish, R. V., Thamban, N. M., Rastogi, N. & Tripathi, S. N. Absorbing refractive index and direct radiative forcing of atmospheric brown carbon over gangetic plain. *ACS Earth Space Chem.* **2**, 31–37 (2018).
31. Chen, P. et al. Light absorption properties of elemental carbon (EC) and water-soluble brown carbon (WS–BrC) in the Kathmandu Valley, Nepal: a 5-year study. *Environ. Pollut.* **261**, 114239 (2020).
32. Rajeev, P., Choudhary, V., Chakraborty, A., Singh, G. K. & Gupta, T. Light absorption potential of water-soluble organic aerosols in the two polluted urban locations in the central Indo-Gangetic plain. *Environ. Pollut.* **314**, 120228 (2022).
33. Pöschl, U. Atmospheric aerosols: composition, transformation, climate and health effects. *Angew Chem. Int. Ed.* **44**, 7520–7540 (2005).
34. Von Schneidemesser, E. et al. Chemistry and the linkages between air quality and climate change. *Chem. Rev.* **115**, 3856–3897 (2015).
35. Mahilang, M., Deb, M. K. & Pervez, S. Biogenic secondary organic aerosols: A review on formation mechanism, analytical challenges and environmental impacts. *Chemosphere* **262**, 127771 (2021).
36. Brown, R. J. & Edwards, P. R. Measurement of anions in ambient particulate matter by ion chromatography: a novel sample Preparation technique and development of a generic uncertainty budget. *Talanta* **80**, 1020–1024 (2009).
37. Friman, M. et al. Long-term characterization of organic and elemental carbon at three different background areas in Northern Europe. *Atmos. Environ.* **310**, 119953 (2023).
38. Widory, D. Combustibles, fuels and their combustion products: a view through carbon isotopes. *Combust. Theor. Model.* **10**, 831–841 (2006).
39. Irei, S. et al. Flow reactor studies of the stable carbon isotope composition of secondary particulate organic matter generated by OH-radical-induced reactions of toluene. *Atmos. Environ.* **40**, 5858–5867 (2006).
40. Kirillova, E. N. et al. 13 C-and 14 C-based study of sources and atmospheric processing of water-soluble organic carbon (WSOC) in South Asian aerosols. *J. Geophys. Res. Atmos.* **118**, 614–626 (2013).
41. Bikkina, S. et al. Dual carbon isotope characterization of total organic carbon in wintertime carbonaceous aerosols from Northern India. *J. Geophys. Res. Atmos.* **121**, 4797–4809 (2016).
42. Bikkina, S. et al. Carbon isotope-constrained seasonality of carbonaceous aerosol sources from an urban location (Kanpur) in the Indo-Gangetic plain. *J. Geophys. Res. Atmos.* **122**, 4903–4923 (2017).
43. Martinsson, J. et al. Evaluation of δ13C in carbonaceous aerosol source apportionment at a rural measurement site. *Aerosol Air Qual. Res.* **17**, 2081–2094 (2017).
44. Górka, M., Kosztowniak, E., Lewandowska, A. U. & Widory, D. Carbon isotope compositions and TC/OC/EC levels in atmospheric PM10 from lower Silesia (SW Poland): Spatial variations, seasonality, sources and implications. *Atmos. Pollut Res.* **11**, 1099–1114 (2020).
45. Singh, G. K. et al. Understanding the origin of carbonaceous aerosols during periods of extensive biomass burning in Northern India. *Environ. Pollut.* **270**, 116082 (2021).
46. Singh, G. K., Rajeev, P., Paul, D. & Gupta, T. Chemical characterization and stable nitrogen isotope composition of nitrogenous component of ambient aerosols from Kanpur in the Indo-Gangetic plains. *Sci. Total Environ.* **763**, 143032 (2021).
47. Bikkina, P., Bikkina, S., Kawamura, K., Sarma, V. V. S. S. & Deshmukh, D. K. Unraveling the sources of atmospheric organic aerosols over the Arabian Sea: insights from the stable carbon and nitrogen isotopic composition. *Sci. Total Environ.* **827**, 154260 (2022).
48. Singh, G. K., Rajeev, P., Paul, D. & Gupta, T. Insights into sources and atmospheric processing at two polluted urban locations in the Indo-Gangetic plains from stable carbon and nitrogen isotope ratios and polycyclic aromatic hydrocarbons in ambient PM2.5. *Atmos. Environ.* **271**, 118904 (2022).
49. Fisseha, R. et al. Determination of primary and secondary sources of organic acids and carbonaceous aerosols using stable carbon isotopes. *Atmos. Environ.* **43**, 431–437 (2009).
50. Fu, P. Q. et al. Diurnal variations of organic molecular tracers and stable carbon isotopic composition in atmospheric aerosols over Mt. Tai in the North China plain: an influence of biomass burning. *Atmos. Chem. Phys.* **12**, 8359–8375 (2012).
51. Cao, J. J. et al. Stable carbon isotopes in aerosols from Chinese cities: influence of fossil fuels. *Atmos. Environ.* **45**, 1359–1363 (2011).
52. Bosch, C. et al. Source-diagnostic dual-isotope composition and optical properties of water-soluble organic carbon and elemental carbon in the South Asian outflow intercepted over the Indian ocean. *J. Geophys. Res. Atmos.* **119**, 11–743 (2014).
53. Kundu, S. & Kawamura, K. Seasonal variations of stable carbon isotopic composition of bulk aerosol carbon from Gosan site, Jeju Island in the East China sea. *Atmos. Environ.* **94**, 316–322 (2014).
54. Ulevicius, V. et al. Fossil and non-fossil source contributions to atmospheric carbonaceous aerosols during extreme spring grassland fires in Eastern Europe. *Atmos. Chem. Phys.* **16**, 5513–5529 (2016).
55. Meusinger, C. et al. Chemical and isotopic composition of secondary organic aerosol generated by α-pinene ozonolysis. *Atmos. Chem. Phys.* **17**, 6373–6391 (2017).
56. Dasari, S. et al. Source quantification of South Asian black carbon aerosols with isotopes and modeling. *Environ. Sci. Technol.* **54**, 11771–11779 (2020).
57. Garbarienė, I. et al. Identification of wintertime carbonaceous fine particulate matter (PM2.5) sources in Kaunas, Lithuania using polycyclic aromatic hydrocarbons and stable carbon isotope analysis. *Atmos. Environ.* **237**, 117673 (2020).
58. Rastogi, N. et al. Chemical and isotopic characteristics of PM10 over the Bay of Bengal: effects of continental outflow on a marine environment. *Sci. Total Environ.* **726**, 138438 (2020).
59. Zenker, K. et al. δ13C signatures of organic aerosols: measurement method evaluation and application in a source study. *J. Aerosol Sci.* **145**, 105534 (2020).
60. Morera-Gomez, Y., Cong, Z. & Widory, D. Carbonaceous fractions contents and carbon stable isotope compositions of aerosols collected in the atmosphere of Montreal (Canada): seasonality, sources, and implications. *Front. Environ. Sci.* **9**, 622521 (2021).
61. Major, I. et al. Detailed carbon isotope study of PM2.5 aerosols at urban background, suburban background and regional background sites in Hungary. *Atmosphere* **13**, 716 (2022).
62. Masalaite, A. et al. Seasonal observation and source apportionment of carbonaceous aerosol from a forested rural site (Lithuania). *Atmos. Environ.* **272**, 118934 (2022).
63. Shen, M. et al. Distribution and stable carbon isotopic composition of Dicarboxylic acids, Ketocarboxylic acids, and α-dicarbonyls in fresh and aged biomass burning aerosols. *Atmos. Chem. Phys.* **22**, 7489–7504 (2022).

64. Lao, Q. et al. Winter monsoon brings substantial terrestrial aerosols to Bay of Bengal and adjacent Indian Ocean: insights from carbon and nitrogen isotopes. *Atmos Environ* 120555 (2024).
65. Ballentine, D. C. et al. Compound-specific isotope analysis of fatty acids and polycyclic aromatic hydrocarbons in aerosols: implications for biomass burning. *Org. Geochem.* **25**, 97–104 (1996).
66. Sang, X. F. et al. Chemical stability of Levoglucosan: an isotopic perspective. *Geophys. Res. Lett.* **43**, 5419–5424 (2016).
67. Mkoma, S. L. et al. Stable carbon and nitrogen isotopic compositions of tropical atmospheric aerosols: sources and contribution from burning of C3 and C4 plants to organic aerosols. *Tellus B Chem. Phys. Meteorol.* **66**, 20176 (2014).
68. Garbaras, A. et al. Stable carbon fractionation in size-segregated aerosol particles produced by controlled biomass burning. *J. Aerosol Sci.* **79**, 86–96 (2015).
69. Cao, F. et al. Inorganic markers, carbonaceous components, and stable carbon isotope from biomass burning aerosols in Northeast China. *Sci. Total Environ.* **572**, 1244–1251 (2016).
70. Masalaite, A. et al. Sources and atmospheric processing of size-segregated aerosol particles revealed by stable carbon isotope ratios and chemical speciation. *Environ. Pollut.* **240**, 286–296 (2018).
71. Song, J. et al. Influence of biomass burning on atmospheric aerosols over the Western South China Sea: insights from ions, carbonaceous fractions, and stable carbon isotope ratios. *Environ. Pollut.* **242**, 1800–1809 (2018).
72. Vernooij, R. et al. Stable carbon isotopic composition of biomass burning emissions–implications for estimating the contribution of C3 and C4 plants. *Atmos. Chem. Phys. Discuss.* 1–35 (2021).
73. Khundadze, N. et al. Benchmarking source-specific isotopic ratios of Levoglucosan to better constrain the contribution of domestic heating to air pollution. *Atmos. Environ.* **268**, 118842 (2022).
74. Gustafsson, O. et al. Brown clouds over South Asia: biomass or fossil fuel combustion? *Science* **323**, 495–498 (2009).
75. Dasari, S. & Widory, D. Radiocarbon (14 C) analysis of carbonaceous aerosols: revisiting the existing analytical techniques for isolation of black carbon. *Front. Environ. Sci.* **10**, 907467 (2022).
76. Zhao, H. et al. Source apportionment of carbonaceous aerosol using dual-carbon isotopes (13 C and 14 C) and Levoglucosan in three Northern Chinese cities during 2018–2019. *Atmos. Chem. Phys.* **22**, 6255–6274 (2022).
77. Ni, H. et al. Non-fossil origin explains the large seasonal variation of highly processed organic aerosol in the northeastern Tibetan Plateau (3,200 m asl). *Geophys. Res. Lett.* 50, eGL104710 (2023).
78. Xu, B. et al. Fates of secondary organic aerosols in the atmosphere identified from compound-specific dual-carbon isotope analysis of oxalic acid. *Atmos. Chem. Phys.* **23**, 1565–1578 (2023).
79. Gensch, I., Kiendler-Scharr, A. & Rudolph, J. Isotope ratio studies of atmospheric organic compounds: principles, methods, applications, and potential. *Int. J. Mass. Spectrom.* **365**, 206–221 (2014).
80. Kirillova, E. N. et al. Water-soluble organic carbon aerosols during a full new Delhi winter: Isotope-based source apportionment and optical properties. *J. Geophys. Res. Atmos.* **119**, 3476–3485 (2014).
81. Agnihotri, R. et al. Stable isotopic and chemical characteristics of bulk aerosols during winter and summer seasons at a station in Western Coast of India (Goa). *Aerosol Air Qual. Res.* **15**, 888–900 (2015).
82. Zhang, W. et al. High time-resolved measurement of stable carbon isotope composition in water-soluble organic aerosols: method optimization and a case study during winter haze in Eastern China. *Atmos. Chem. Phys.* **19**, 11071–11087 (2019).
83. Vodička, P., Kawamura, K., Schwarz, J. & Žímal, V. Seasonal changes in stable carbon isotopic composition in the bulk aerosol and gas phases at a suburban site in Prague. *Sci. Total Environ.* **803**, 149767 (2022).
84. Lekinwala, N. L. et al. A framework for setting up a country-wide network of regional surface PM2.5 sampling sites utilising a satellite-derived proxy – the COALESCE project, India. *Atmos. Environ.* **234**, 117544 (2020).
85. Maheshwarkar, P. et al. Understanding the influence of meteorology and emission sources on PM2.5 mass concentrations across India: First results from the COALESCE network. *J. Geophys. Res. Atmos.* 127, eJD035663 (2022).
86. Qadri, A. M. et al. Variabilities of δ13C and carbonaceous components in ambient PM2.5 in Northeast India: insights into sources and atmospheric processes. *Environ. Res.* **214**, 113801 (2022).
87. Rabha, S. et al. Year-long evaluation of aerosol chemistry and meteorological implications of PM2.5 in an urban area of the Brahmaputra Valley, India. *Environ. Sci. Atmos.* **3**, 196–206 (2023).
88. Yadav, K. et al. Tracing the predominant sources of carbon in PM2.5 using δ13C values together with OC/EC and select inorganic ions over two COALESCE locations. *Chemosphere* **308**, 136420 (2022).
89. Dhandapani, A. et al. Characterization of fine particulate matter water-soluble inorganic ions and Estimation of aerosol acidity at three COALESCE network sites—Mysuru, Bhopal, and Mesra—in India. *Environ. Sci. Pollut Res.* **30**, 69241–69257 (2023).
90. Haswani, D. et al. Pollution characteristics and ecological risks of trace elements in PM2.5 over three COALESCE network sites—Bhopal, Mesra, and Mysuru, India. *Chemosphere* **324**, 138203 (2023).
91. Mukherjee, S. et al. PM2.5 pollution exceeding Indian standard over a semi-urban region at Eastern IGP: chemistry, meteorological impact, and long-range transport. *Sci. Total Environ.* **898**, 165415 (2023).
92. Singh, G. K. et al. Investigation of sources and atmospheric transformation of carbonaceous aerosols from Shyamnagar, Eastern Indo-Gangetic plains: insights from δ13C and carbon fractions. *Chemosphere* **326**, 138422 (2023).
93. Singh, G. K., Rajput, P., Paul, D. & Gupta, T. Wintertime study on bulk composition and stable carbon isotope analysis of ambient aerosols from North India. *J. Aerosol Sci.* **126**, 231–241 (2018).
94. Paul, D., Skrzypek, G. & Fórizs, I. Normalization of measured stable isotopic compositions to isotope reference scales—a review. *Rapid Commun. Mass. Spectrom.* **21**, 3006–3014 (2007).
95. Jones, N. L., Davis, R. J. & Sabbah, W. A comparison of three-dimensional interpolation techniques for plume characterization. *Groundwater* **41**, 411–419 (2003).
96. Khouni, I., Louhichi, G. & Ghrabi, A. Use of GIS-based inverse distance weighted interpolation to assess surface water quality: case of Wadi El Bey, Tunisia. *Environ. Technol. Innov.* **24**, 101892 (2021).
97. Smith, B. N. & Epstein, S. Two categories of 13 C/12 C ratios for higher plants. *Plant. Physiol.* **47**, 380–384 (1971).
98. Sudheer, A. K. et al. Carbonaceous aerosol over semi-arid region of Western India: heterogeneity in sources and characteristics. *Atmos. Res.* **178**, 268–278 (2016).
99. Sharma, S. K. et al. Variation of stable carbon and nitrogen isotopic composition of PM10 at urban sites of Indo-Gangetic plain (IGP) of India. *Bull. Environ. Contam. Toxicol.* **95**, 661–669 (2015).
100. Widory, D. et al. The origin of atmospheric particles in Paris: a view through carbon and lead isotopes. *Atmos. Environ.* **38**, 953–961 (2004).
101. Pavuluri, C. M. & Kawamura, K. Evidence for 13-carbon enrichment in oxalic acid via iron-catalyzed photolysis in aqueous phase. *Geophys. Res. Lett.* **39**, L03802 (2012).
102. Irei, S., Rudolph, J., Huang, L., Auld, J. & Hastie, D. Stable carbon isotope ratio of secondary particulate organic matter formed by photooxidation of toluene in indoor smog chamber. *Atmos. Environ.* **45**, 856–862 (2011).
103. Roy, S. et al. Wintertime aerosol properties of urban desert region of Western India: implications in regional climate assessment. *Sci. Total Environ.* **868**, 161473 (2023).
104. Agnihotri, R. et al. Stable carbon and nitrogen isotopic composition of bulk aerosols over India and Northern. *Indian Ocean. Atmos Environ.* **45**, 2828–2835 (2011).
105. Masalaite, A. et al. Seasonal changes of sources and volatility of carbonaceous aerosol at urban, coastal, and forest sites in Eastern Europe (Lithuania). *Atmos. Environ.* **225**, 117374 (2020).

106. Pavuluri, C. M. & Kawamura, K. Enrichment of 13 C in Diacids and related compounds during photochemical processing of aqueous aerosols: new proxy for organic aerosols aging. *Sci. Rep.* **6**, 36467 (2016).
107. Keeling, C. D. The concentration and isotopic abundances of atmospheric carbon dioxide in rural areas. *Geochim. Cosmochim. Acta*. **13**, 322–334 (1958).
108. Ceburnis, D. et al. Quantification of the carbonaceous matter origin in submicron marine aerosol by 13 C and 14 C isotope analysis. *Atmos. Chem. Phys.* **11**, 8593–8606 (2011).
109. Phillips, D. L. & Gregg, J. W. Source partitioning using stable isotopes: coping with too many sources. *Oecologia* **136**, 261–269 (2003).
110. Wu, Y. et al. Composition and sources of aerosol organic matter in a highly anthropogenic influenced semi-enclosed Bay: insights from excitation-emission matrix spectroscopy and isotopic evidence. *Atmos. Res.* **241**, 104958 (2020).
111. Gu, W. et al. Marine fresh carbon pool dominates summer carbonaceous aerosols over Arctic Ocean. *J. Geophys. Res. Atmos.* 128, eJD037692 (2023).
112. Attri, P. et al. Atmospheric aerosol chemistry and source apportionment of PM10 using stable carbon isotopes and PMF modelling during fireworks over Hyderabad, Southern India. *Heliyon* **10**, e15732 (2024).
113. Aggarwal, S. G. et al. Organic and inorganic markers and stable C-, N-isotopic compositions of tropical coastal aerosols from megacity Mumbai: sources of organic aerosols and atmospheric processing. *Atmos. Chem. Phys.* **13**, 4667–4680 (2013).
114. Byers, L. et al. A global database of power plants. *World Resour. Institute* **18**, (2018).
115. Tkachenko, N. et al. Global database of cement production assets and upstream suppliers. *Sci. Data*. **10**, 696 (2023).
116. Sawlani, R., Agnihotri, R. & Sharma, C. Chemical and isotopic characteristics of PM2.5 over new Delhi from September 2014 to May 2015: evidence for synergy between air pollution and meteorological changes. *Sci. Total Environ.* **763**, 142966 (2021).
117. Pavuluri, C. M., Kawamura, K., Swaminathan, T. & Tachibana, E. Stable carbon isotopic compositions of total carbon, Dicarboxylic acids, and Glyoxylic acid in the tropical Indian aerosols: implications for sources and photochemical processing of organic aerosols. *J. Geophys. Res. Atmos.* **116**, D18305 (2011).
118. López-Veneroni, D. The stable carbon isotope composition of PM2.5 and PM10 in Mexico City metropolitan area air. *Atmos. Environ.* **43** (29), 4491–4502 (2009).
119. Kunwar, B., Kawamura, K. & Zhu, C. Stable carbon and nitrogen isotopic compositions of ambient aerosols collected from Okinawa Island in the Western North Pacific Rim, an outflow region of Asian dusts and pollutants. *Atmos. Environ.* **131**, 243–253 (2016).

Acknowledgements

This study was carried out with financial support from the Ministry of Environment, Forest and Climate Change (MoEFCC), Government of India under the National Carbonaceous Aerosols Programme (NCAPCOALESCE) [Grant 14/10/2014-CC(Vol.II)]. We thank three anonymous reviewers for their thorough reviews, which led to important clarifications. Editorial handling by Bomidi Lakshmi Madhavan and Rafal Marszalek (Chief Editor) is appreciated.

Author contributions

DP: Funding acquisition, Supervision in stable isotope analysis and interpretation, Conceptualization, Investigation, Writing – original draft. GKS: Investigation, Data Analysis and interpretation, Literature review, Writing – original draft. TG: Funding acquisition, Supervision, Writing – review and editing. AC: Sampling Resources. BKS: Sampling Resources, Writing – review and editing. RSR: Sampling Resources, Writing – review and editing. GH: Sampling Resources. HP: Sampling Resources. CV: Sampling Resources.

Declarations

Competing interests

The authors declare no competing interests.

Additional information

Supplementary Information The online version contains supplementary material available at https://doi.org/10.1038/s41598-025-03987-5.

Correspondence and requests for materials should be addressed to D.P. or G.K.S.